

MIT Open Access Articles

*Sub-wavelength plasmonic readout for
direct linear analysis of optically tagged DNA*

The MIT Faculty has made this article openly available. **Please share** how this access benefits you. Your story matters.

Citation: Varsanik, Jonathan et al. "Sub-wavelength plasmonic readout for direct linear analysis of optically tagged DNA." Plasmonics in Biology and Medicine VII. Ed. Tuan Vo-Dinh & Joseph R. Lakowicz. ©2010 SPIE

As Published: <http://dx.doi.org/10.1117/12.841165>

Publisher: SPIE

Persistent URL: <http://hdl.handle.net/1721.1/58612>

Version: Final published version: final published article, as it appeared in a journal, conference proceedings, or other formally published context

Terms of Use: Article is made available in accordance with the publisher's policy and may be subject to US copyright law. Please refer to the publisher's site for terms of use.



Sub-Wavelength Plasmonic Readout for Direct Linear Analysis of Optically Tagged DNA

Jonathan Varsanik,^{A,B} William Teynor,^B John LeBlanc,^B Heather Clark,^B Jeffrey Krogmeier,^C Tian Yang,^D Kenneth Crozier,^D Jonathan Bernstein*^B

^AMassachusetts Institute of Technology, 77 Massachusetts Ave. Cambridge, MA 02139

^BCharles Stark Draper Laboratory, 555 Technology Square, Cambridge MA 02139

^CU.S. Genomics, 12 Gill St. Suite 4700 Woburn, MA 01801

^DSchool of Engineering and Applied Sciences, Harvard University, Cambridge, MA 02138

ABSTRACT

This work describes the development and fabrication of a novel nanofluidic flow-through sensing chip that utilizes a plasmonic resonator to excite fluorescent tags with sub-wavelength resolution. We cover the design of the microfluidic chip and simulation of the plasmonic resonator using Finite Difference Time Domain (FDTD) software. The fabrication methods are presented, with testing procedures and preliminary results.

This research is aimed at improving the resolution limits of the Direct Linear Analysis (DLA) technique developed by US Genomics [1]. In DLA, intercalating dyes which tag a specific 8 base-pair sequence are inserted in a DNA sample. This sample is pumped through a nano-fluidic channel, where it is stretched into a linear geometry and interrogated with light which excites the fluorescent tags. The resulting sequence of optical pulses produces a characteristic “fingerprint” of the sample which uniquely identifies any sample of DNA. Plasmonic confinement of light to a 100 nm wide metallic nano-stripe enables resolution of a higher tag density compared to free space optics. Prototype devices have been fabricated and are being tested with fluorophore solutions and tagged DNA. Preliminary results show evanescent coupling to the plasmonic resonator is occurring with 0.1 micron resolution, however light scattering limits the S/N of the detector. Two methods to reduce scattered light are presented: index matching and curved waveguides.

Keywords: Plasmon resonance, optical waveguide, microfluidics, sub-wavelength resolution

1. INTRODUCTION

Surface plasmonic resonance is a collective oscillation of electrons that occurs on a metal surface. This resonance may occur at optical frequencies, and has a characteristic wavelength which is small compared to the free-space optical wavelength. The ability to confine an intense electromagnetic field to a sub-wavelength region on a metal surface has been used to excite fluorescent molecules [2]. Not only is the wavelength of the surface plasmon smaller than the free-space wavelength at that frequency, but the field is enhanced, strongly confined to the surface, and exponentially decaying away from the surface [3]. These characteristics make the surface plasmon a useful tool for high resolution sensing very close to the metal surface.

In this work, we introduce light through an optical waveguide in BK7 glass which has an index of refraction of 1.51. Strong energy transfer from optical waveguide to plasmon waveguide only occurs when the k-vectors are matched at a given frequency. The plasmon mode with its large k vector cannot directly absorb or radiate free space light, but it can excite nearby fluorophores. Light is coupled from the optical waveguide to a non-radiating mode on a sub-micron stripe of metal, thereby confining light to a region much shorter than its wavelength. This width is limited only by nanofabrication technology, and should be scalable at least down to 20 nm. This sub-wavelength region can be used to excite fluorophores on tagged biomolecules as they flow through the system (Figure 1) with higher resolution than would be possible using free-space optics.

*jbernstein@draper.com; phone 617 258-2513, fax 617 258 4238; www.draper.com

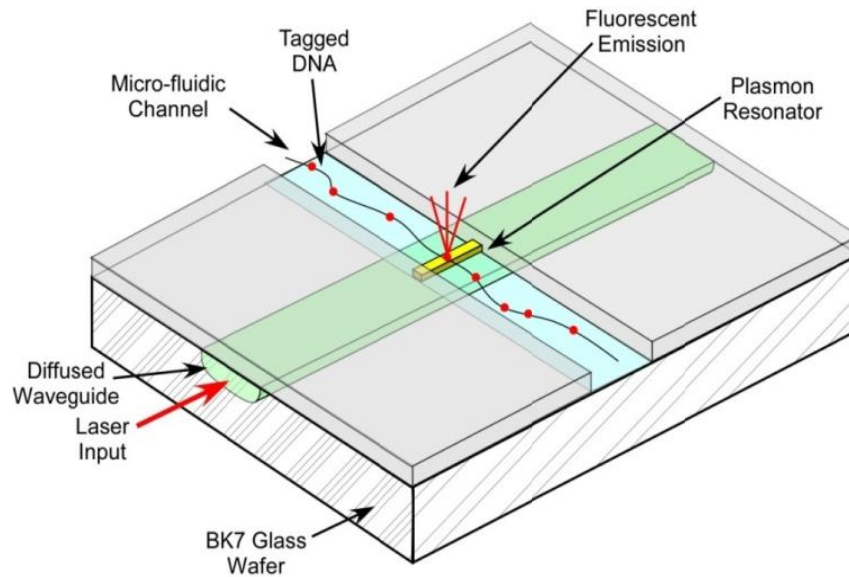


Figure 1. Cartoon of detection scheme. Microfluidic channel carries stretched, tagged DNA past a plasmonic resonator (stripe of metal) coupling optical energy from a diffused optical waveguide.

2. PLASMONIC RESONATOR DESIGN

The dispersion of the plasmonic resonance of a metal stripe is determined by the material properties and dimensions of the metal and surrounding dielectric. To ensure effective coupling at the wavelengths of interest, the plasmonic resonator should be designed to match k vector (wavelength) with the underlying optical waveguide. The simulation of the plasmonic resonator was carried out using a Finite Difference Time Domain (FDTD) simulation program FULLWave from Rsoft. FDTD simulation engines are able to predict the electromagnetic response of a system by solving Maxwell's equations on a spatial grid. With a given initial and boundary conditions, the electric fields are calculated on every point in the grid, and the magnetic fields are calculated in between each of these points. The fields are progressed by a given time step, and the new fields are calculated over the spatial grid. Through this process, one can determine the behavior of arbitrary geometries to electromagnetic fields.

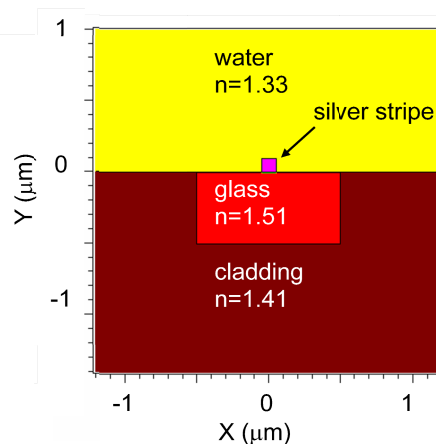


Figure 2. Simulated plasmonic stripe: Metal stripe on waveguide, cross section through 100 nm X 100 nm stripe. Au and Al stripe dimensions are identical. Actual BK-7 glass cladding has $n \cong 1.51$, but large Δn was assumed to confine the mode and reduce the simulation volume and time.

To ensure accurate simulations, the spacing of the grid points and the time step must be small enough to resolve the details of the waves of interest. For a system with nano-sized features at optical frequencies, this can lead to memory and computation intensive calculations.

Using the FDTD method, plasmon dispersion diagrams for a 100x100 nm X 10 um long metal stripe on a glass diffused waveguide were calculated, as shown in Figure 2 for 3 candidate metals (Au, Ag and Al). To reduce the simulation volume, the refractive index of the cladding is artificially reduced to 1.41 to give stronger confinement of the EM field around the waveguide. In the actual diffused waveguide, the index change is only about 0.03 for a silver diffused waveguide.

Figure 3 shows the calculated frequency vs. k ($2\pi/\lambda$) diagram for the surface plasmon modes on a thin strip of various metals, as well as the light-line for the BK7 glass waveguide. Energy must transfer from the waveguide to the water-metal interface for the device to work properly. Strong energy transfer occurs when the lines of those respective modes cross on the omega-k diagram, indicating that at that frequency the wavelengths match.

US Genomics has used laser wavelengths of 633 (He-Ne) nm, 532 nm (Nd-YAG) and 442 nm (He-Cd) to detect specific fluorophore tags intercalated in DNA. For example, 442 nm excites the POPO-1 molecule, whereas 532 nm excites either the ATTO or the TAMRA molecules [4]. We would like to be able to design a plasmon resonator to match the BK7 waveguide mode at each of these free-space wavelengths (frequencies). However, the predicted plasmon wavelengths are not a good match for these 3 laser wavelengths.

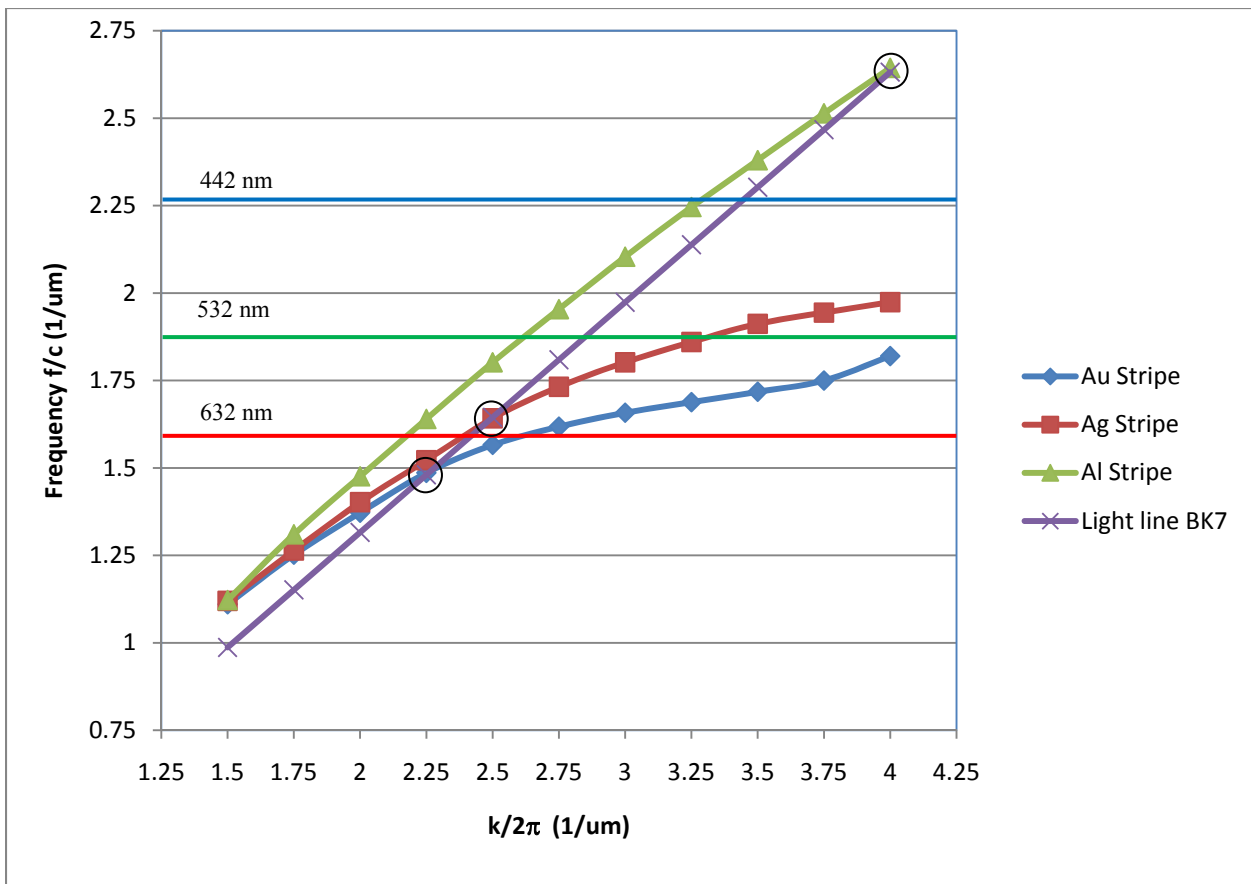


Figure 3. Dispersion relation of the water-metal surface modes of a 100nm x 100nm cross-section plasmonic resonator. Curves for Au, Ag and Al are shown. Also shown is light line for BK7 glass, $n = 1.52$, and 3 laser wavelengths. Good energy coupling from optical waveguide to plasmon modes is predicted at the intersections of the BK7 light-line with the various plasmon curves, shown with open circles.

Table 1 lists the free-space wavelengths at which each of the 3 metals are calculated to couple optimally from the plasmon mode to the glass waveguide. Aluminum couples well at 380 nm, in the near UV. Ag is a good match at 610 nm, near the He-Ne wavelength. Au is a good match at 676 nm.

Table 1. Plasmon mode intersections and common laser wavelengths

Metal	Intersection λ (um)	Laser Wavelengths	Laser
Au	0.676	0.633	red (HeNe)
Ag	0.610	0.532	green (Nd-YAG)
Al	0.380	0.442	blue (He-Cd)

Many other laser sources are available at different frequencies and many other fluorophores are available to match these wavelengths. The optimal system will need to match the plasmon resonance to the laser source and fluorophore.

2.1 Channel Design

The design for the nanofluidic channels (Figure 4) was provided by US Genomics. These channels contain three funnel shaped hydrodynamic stretching regions that stretch the segments of DNA, ensuring that it is in a linear configuration when it passes through the interrogation area. The hydrodynamic stretching regions were designed by the Doyle group at MIT [5]. Side ports are used to introduce additional sheath fluid and increase the stretching of the DNA.

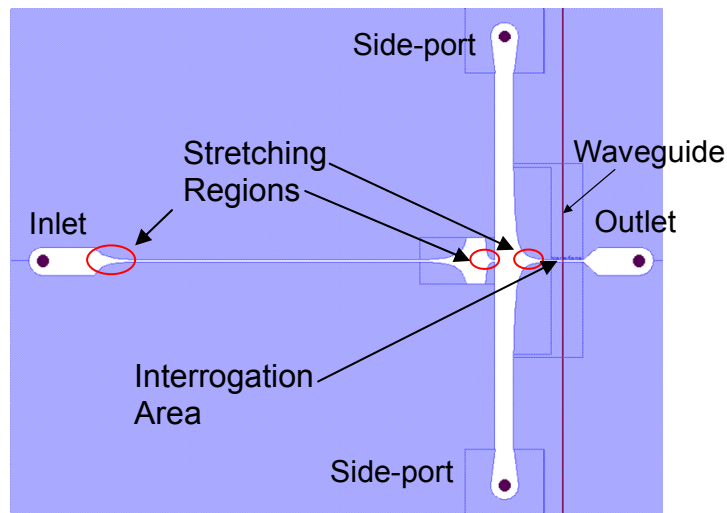


Figure 4. Fluidic layout of the sensor chip.

3. FABRICATION

The microfluidic chips are fabricated on 100 mm wafers of Schott BK-7 glass using mostly processes available in a standard MEMS fabrication facility. BK-7 glass was chosen as the substrate due to its high optical purity and strength, and availability of processes to diffuse high quality optical waveguides. The fabrication process is shown in Figure 5.

The starting BK-7 wafer (0.5 mm thick x 100 mm diameter) is cleaned with a sulfuric acid/hydrogen peroxide “Piranha” solution. A standard liftoff procedure is used to pattern 200 Å of Ta on the wafer for alignment marks. These marks are used for aligning subsequent photomask steps.

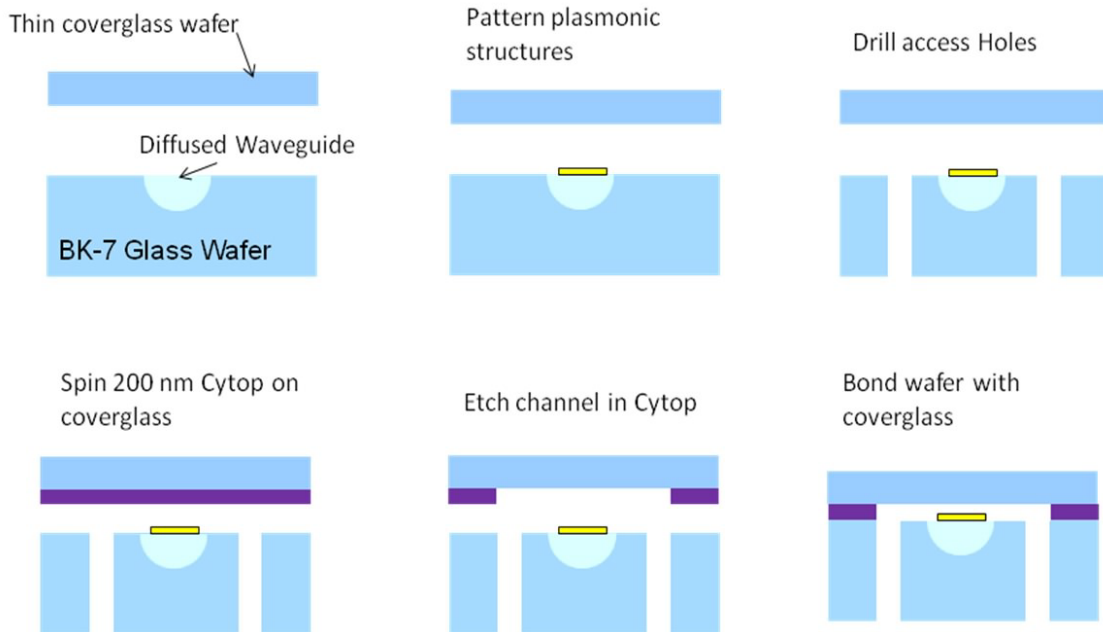


Figure 5. Fabrication process overview.

Waveguides are next added to the wafer. This process is detailed in the following section on waveguides. After the waveguides are added, the plasmonic resonators are defined. This is accomplished by spinning on 200 nm of PMMA e-beam resist, then coating with ESPACER 300 (Showa Denko), a conductive polymer, to prevent charging. The PMMA is exposed with an electron beam lithography tool (RAITH 150) at the Massachusetts Institute of Technology SEBL facility. The PMMA is developed in 2:1 MIBK:IPA and rinsed in IPA, after which 10nm of Cr and 100 nm of Au are deposited in an E-beam evaporation tool. After lifting off the Cr/Au, the plasmonic resonators are complete (Figure 6).

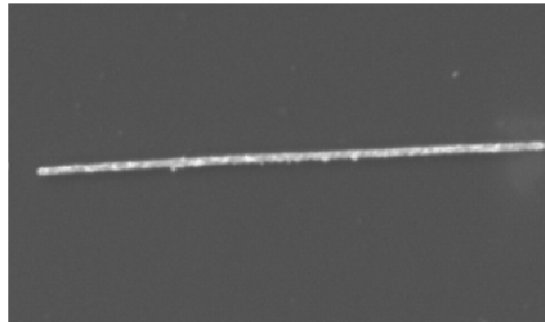


Figure 6. SEM of plasmonic resonator. Au stripe is 160 nm wide X 100 nm thick X 10 μ m long.

The wafers are then sent out to US Photonics (<http://usphotonics.net/>) to have microfluidic input and output holes drilled using a femto-second laser. After the holes are drilled the wafers are re-cleaned and bonded to a thin coverslip (200 μ m thick x 100mm diameter, also made of BK-7), using a fluorocarbon polymer called CYTOP [6-8]. Microfluidic channels are etched into the CYTOP layer using a photoresist mask and oxygen plasma etch. After the wafer is bonded to the coverslip, the bonded pair is diced into chips. The sides of the chip that intersect the optical waveguide are optically polished and a fiber optic pigtail is attached with Norland UV curing adhesive. The chips are now ready to test.

A few of the fabrication steps are described in more detail in the following sections.

3.1 Optical Waveguides

There are many technologies and material systems used to fabricate optical waveguides, including glass waveguides made by chemical vapor deposition (CVD), flame hydrolysis deposition (FHD), spin-on glasses, sol gels, ion implantation and ion exchange. In this work, we have chosen ion-exchange waveguides to integrate with our glass microfluidics.

For optical waveguiding, a higher index core is surrounded by a lower index cladding material. In the ion-exchange process, a glass is immersed in a molten alkali salt bath, allowing ions from the bath to exchange with mobile ions in the glass. Often the glass ion is Na^+ as it not only has a high mobility, but also is found in many common soda lime and borosilicate glasses. When the ions exchange, a change in the glass refractive index can occur by two effects. When a smaller ion replaces a larger ion, the glass matrix can collapse around the smaller ion, with the increased index coming from an increase in density. Secondly, if the ion from the bath has a higher electronic polarizability, such as K^+ or Ag^+ compared to Na^+ , there is an increase in the refractive index [9].

There are several variations on the ion exchange process, including thermal exchange from a molten salt, field assisted exchange from a molten salt, field assisted burial and thermally annealing [10]. For this work, we have chosen the $\text{Ag}^+ - \text{Na}^+$ ion exchange system. This system produces a higher index change Δn at a lower diffusion temperature, compared to the $\text{K}^+ - \text{Na}^+$ system. The larger Δn allows tighter bends in the waveguides.

Ion exchanged waveguides were chosen for several reasons. The waveguides are diffused into the surface of a glass wafer, leaving a flat substrate suitable for wafer bonding. The index changes achievable with ion exchanged waveguides make them relatively easy to integrate with fibers.

$\text{Ag}^+ - \text{Na}^+$ ion exchange was masked using a photolithographically patterned 200 nm Al film, leaving open the areas to be ion-exchanged. Wafer backs were also Al coated to prevent wafer bow. The glass wafer with the aluminum masking layer is submerged in a molten AgNO_3 salt bath at 365 °C for 35 minutes. The glass is then cleaned and stripped of the aluminum film. Some wafers were K^+ ion diffused in molten KNO_3 at 385°C for 14 hours.

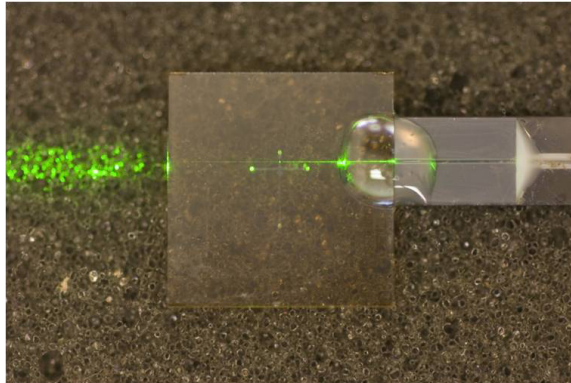


Figure 7. Laser light from a fiber optic cable attached to a device and guided by diffused waveguide out the other side.

3.2 Microfluidic Channel Fabrication

The microfluidic channels are fabricated using a process similar to that described in [6]. A polymer layer is spun onto a glass substrate, that layer is patterned, and then another piece of glass is bonded on top of this layer, sealing the microfluidic channels. In our process, the polymer and channels are made on a thin glass coverslip. A coverslip is used to improve the detection capabilities of our device. With this thin glass, it is possible to use a high magnification, high numerical aperture lens in our tests. The channels are made on the coverslip to ensure that the polymer layer is not damaged by the aggressive processing done to the bottom substrate (laser hole drilling).

3.3 Edge Polishing

Once the chips have been diced, the waveguide ends must be polished. This is accomplished using diamond paper of sequentially smaller size grit, on an Allied Multi-Prep polishing tool. The final grit is 0.5 μm diamond. Care is taken to

protect the entrance holes to the μ fluidic circuit with adhesive tape. A device with a diffused waveguide attached to a fiber optic cable is shown in Figure 7. Light enters from the fiber optic on the right and is guided through the chip to exit on the left.

3.4 Wafer Bond Processes

Several bonding processes have been used to fabricate these microfluidic devices, including polymer bonding with PMMA, glass-glass anodic bonding, and polymer bonding with CYTOP. The desired bond process would have: strong adhesion, temperature $< 350^{\circ}\text{C}$, and cleanable surfaces prior to bonding. The bond process also relates to the fluidic channel formation, since the channels may be formed by patterning the bond layer or by etching channels into one of the glass wafers. The resulting channel should not scatter light from the waveguides, as this reduces the optical S/N of the fluorescent signal. A low temperature bond process is preferred, to minimize changes to the profile of the diffused waveguides and avoid diffusion driven shape changes to the metal plasmonic stripes.

PMMA bonding was found to have marginal adhesion strength. In addition the PMMA surface cannot be rigorously cleaned in solvents or hot acids, leading to particles at the bond interface.

After a literature search, a glass-glass anodic bond process using a “disappearing layer” of Al was found [11]. Performing experiments with Al as well as Ti and amorphous Si, we chose amorphous Si (a-Si) as the bond layer, as it has been used previously to make nanofluidic devices in glass [12,13]. However, this process requires both high temperature (335°C) and an applied voltage, which very likely perturbs the ion diffused waveguide. Channels were etched into the substrate wafer (or in later runs the cap wafer), resulting in a discontinuity in the index of refraction where the waveguide crosses the fluidic channel. This dielectric discontinuity causes considerable light scattering, limiting the fluorescent signal/noise.

Ultimately a new polymer bond process was adopted, using a unique polymer called CYTOP manufactured by Asahi [6-8]. This polymer has outstanding adhesion strength, and an index of refraction very close to water (1.34, vs. 1.33 for water). Hence the evanescent light field from the waveguide sees only $\Delta n=0.01$ as it crosses into a water filled channel, resulting in minimal scattering. Additionally, CYTOP is extremely chemically inert, and can be cleaned rigorously in most solvents and hot acids, leading to low particulate densities at the bond interface.

Bond strength was tested using the razor blade test, shown in Fig. 8. A razor blade is pushed between the two wafers, and the distance that the resulting delaminated area extends beyond the tip of the razor blade is measured, from which the surface energy of the bond can be calculated using the following formula [14]:

$$\gamma = \frac{3 E t_w^3 t_b^2}{32 L^4} \tag{2}$$

where L is the crack extent beyond the razor blade, E is Young’s modulus for the wafers, t_b and t_w are the razor and wafer thicknesses, and γ is the bond energy in J/m^2 . For very strong bonds, the wafers crack before a measurement can be made. CYTOP bonds were sometimes too strong to measure, i.e. the wafers cracked.

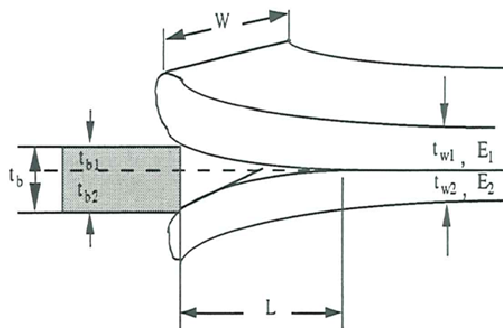


Figure 8: Diagram of razor blade test [14]

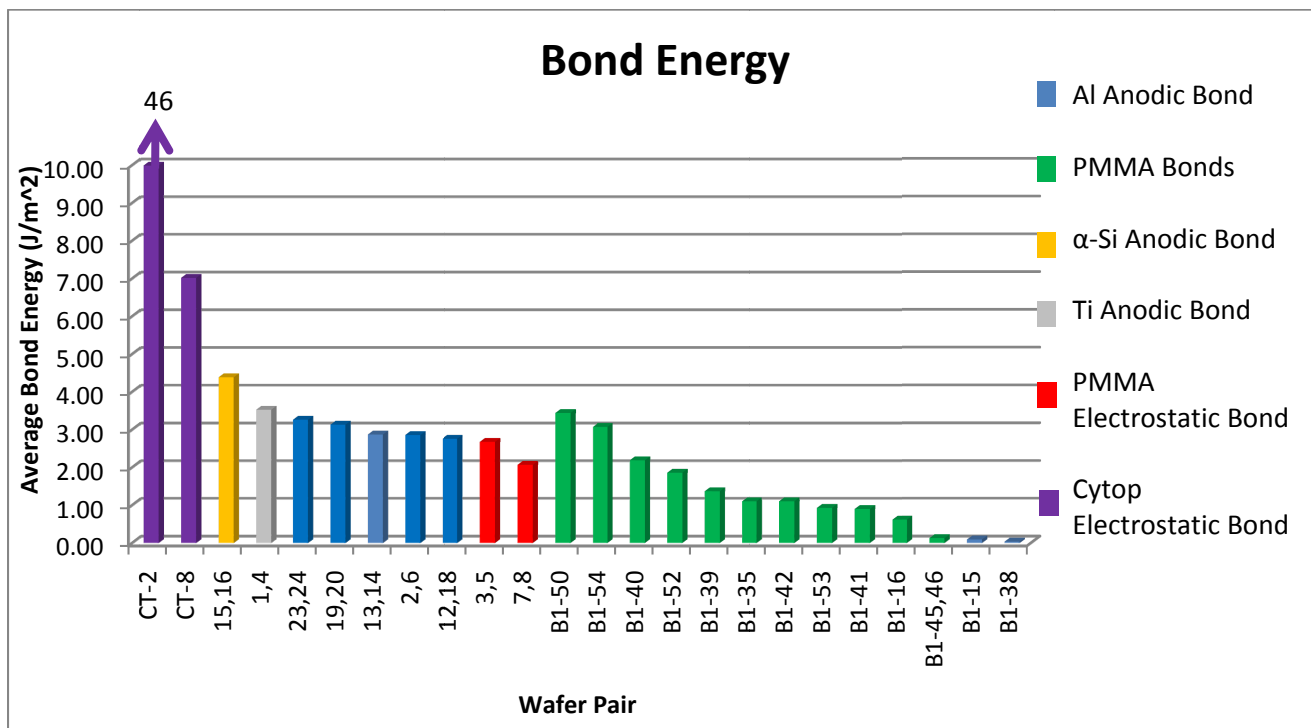


Figure 9. Bar chart showing average bond energy for various wafer bond techniques.

4. TEST

The first step of testing these chips is to fill them with fluid containing fluorophores, and observe if the plasmonic stripe excites fluorescence. Filling a nanofluidic channel presents challenges and hence is addressed below.

4.1 Fluid Filling

Filling the channels of a nanofluidic device is difficult. Due to the high surface/volume ratio of a nanochannel, surface forces dominate the fluid behavior. To force water into a 200 nm deep channel of a non-wetting surface like Teflon would require over 7 atmospheres of pressure. Fortunately the glass surfaces of this channel are somewhat hydrophilic. In general, capillary filling is a preferred method for filling nanofluidic channels [15]. However, we found capillary filling to be slow, unreliable, and not appropriate for a flow-through system. Furthermore, capillary filling is dependent on the viscosity and wetting behavior of the filling liquid. While IPA (isopropyl alcohol) wicks into the channel quickly, it also quickly dewets from many regions of the channel leaving gas voids. This dewetting would usually happen before the channel was entirely filled. Mixing the IPA with water would slow the dewetting process, enabling the channel to be fully filled. Unlike IPA, pure water often would not enter the channels at all.

The alternative to capillary filling is pressure-driven filling. A microfluidic manifold is required to connect to the sensor chip. We used a PDMS (Poly Dimethyl-Siloxane) manifold cut to 1cm x 1cm from a sheet of PDMS about 7.5 mm thick. Figure 10 shows a PDMS manifold connected to a syringe for fluid filling.

The PDMS is cleaned and both the PDMS and chip are placed in an oxygen plasma to activate the surfaces. After plasma activation, the pieces are placed together to form a bond. To allow time to align the PDMS to the chip, a drop of water is placed on the manifold while it is being aligned under an optical microscope. When the pieces are aligned, they are placed on a hotplate, to drive out the water and create the bond. The process must be done within a few minutes after plasma activation for the bond to be effective.

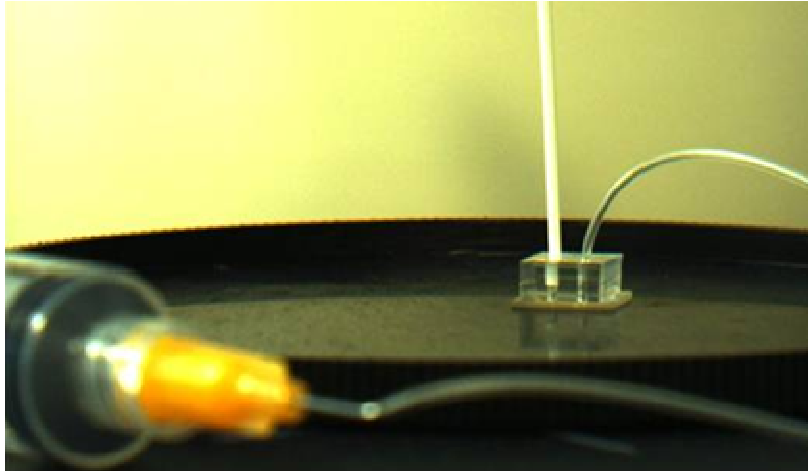


Figure 10: PDMS manifold and syringe attached to a chip.

Thin PDMS tubes are placed in the holes, and then sealed in place with PDMS adhesive. Syringe fittings are fitted into the tubes, and these connections are also sealed with PDMS or a room-temperature-vulcanizing silicone. In most operation, fluid is placed in one of the inlet tubes, and flow is induced by a vacuum applied to the outlet.

4.2 Light Scattering

The initial batch of fabricated devices had high levels of scattered light passing through the detection zone. To enable single molecule imaging, all scattered light must be suppressed. We identified two main sources of scattered light; the waveguide-fluidic channel intersection and fiber-waveguide junction

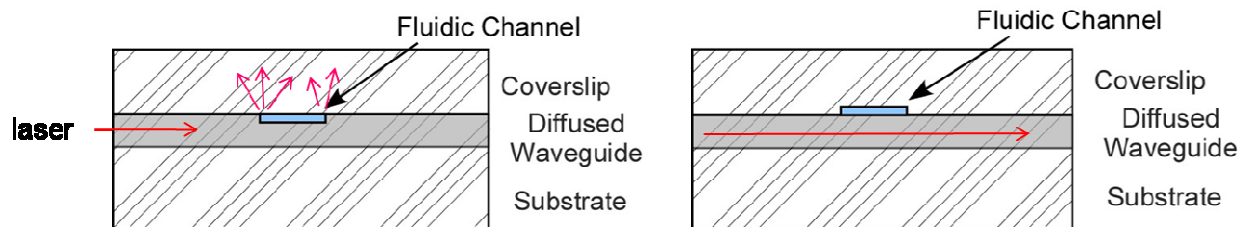


Figure 11. Diagram of cross section of device when the channel was in the wafer (left) and when it was moved to the coverslip (right). Moving the channel into the cover-slip reduces scattering.

When the channel is etched into the substrate wafer, it is also etched into the waveguide (Figure 11). This discontinuity in the profile of the waveguide scatters light, due to the refractive index difference between glass and water. To reduce scattering the channel was moved from the waveguide wafer to the cover slip wafer. FDTD simulations showed this would reduce the intensity of scattered light by 49%. Scattering is not completely eliminated because the evanescent field still sees a discontinuity at the fluidic channel edges. Using a fluidic channel cut into the CYTOP bond layer should eliminate most of this scattering, as the water filled channel has almost the same index as the CYTOP.

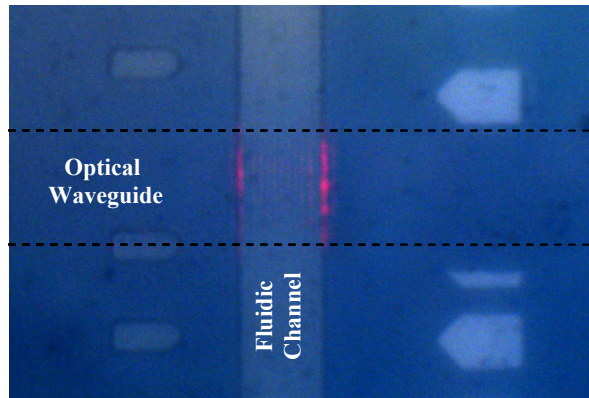


Figure 12. Light scattering where optical waveguide intersects fluidic channel etched into the waveguide.

Another cause of scattered light is the connection point of the fiber optic pigtail to the chip. Because the fiber mode and the waveguide mode are not perfectly matched, there is scattering at this interface. This scattered light reaches the interrogation zone. A newer design uses a 90° waveguide bend to prevent light scattered from the fiber-waveguide connection reaching the detection zone.

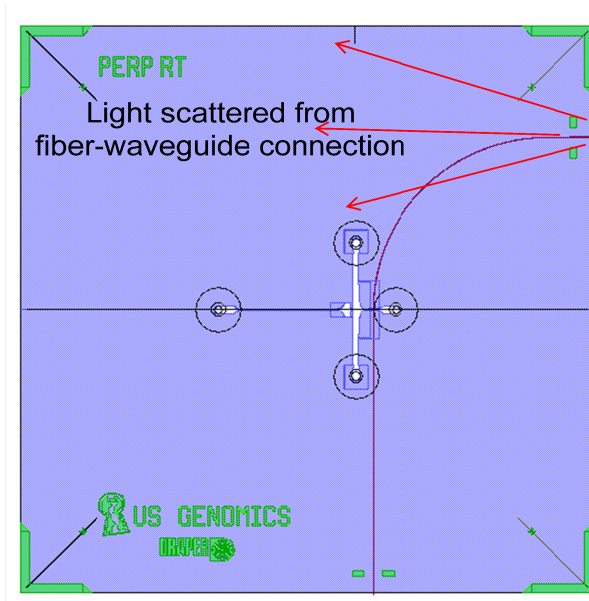


Figure 13. Curved waveguide causes most light escaping from the fiber-waveguide junction to miss the detection zone.

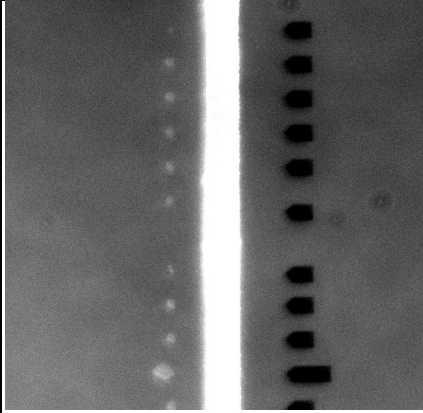
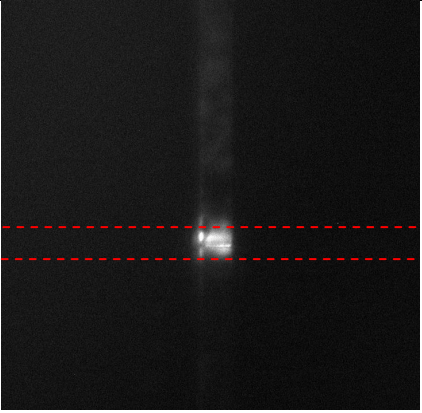
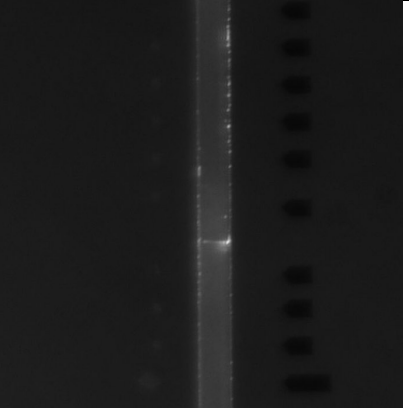
4.3 Fluorescence Imaging

To test for successful coupling between the waveguide and the plasmonic resonator, initial tests were performed using fluorescence imaging. The channel was filled with a 10 mM solution of Alexa Fluor 633 dye in IPA. The chip is observed in a fluorescence microscope (Zeiss Axiovert 200, using Chroma Technology filters HQ615/40x, Q660LP, and HQ675/50m as the excitation, dichroic and emission filters, respectively). After filling the channel with a dye solution, the device can be illuminated with white light from a halogen lamp or filtered light from a mercury arc lamp, and viewed through a variety of filters. Using these two illumination sources, effective filling of the device and proper function of the microscope are verified. In use as a fluorescence microscope, the sample is illuminated with one wavelength of light, which excites the fluorophores that emit light at a slightly shifted wavelength. By observing the device through a filter, the input light is rejected and only fluorescence is observed.

Next, to verify coupling from the waveguide to the plasmonic resonator, the illuminating light is turned off and the input laser is turned on. The laser used was a 635nm wavelength diode pumped solid state laser. If the microscope is properly set up, the input laser light will be rejected by the filters and only light from fluorescing particles will be observed. Therefore, if the plasmonic stripe were working properly a thin stripe should be observed at this point – indicating that the fluorophores above the stripe are being excited by the plasmonic resonator and are emitting enough light to be detected.

Light emission from the plasmonic stripe was observed, however other sources of light were also observed (Figure 14 and 15). Light is seen at the edges of the channel, indicating that scattered light at the edges of the channel is exciting emission from fluorophores in the channel. Although the metal stripe is exciting fluorophores as well, we are unsure if this is merely due to scattered light or if we are getting effective coupling from the waveguide to the plasmon resonator. Scattering must be reduced to clarify the source of the fluorescent signal.

Further evidence in favor of scattering as the source of the fluorescence is observed using fluorescence illumination again. In this mode, by adjusting the contrast of the image, it was possible to see the plasmonic stripe more brightly than the rest of the channel (Fig. 16). This is an unexpected result, as we did not expect white light incident from below to drive the plasmonic resonator to a strong resonance. It is possible that instead of exciting fluorophores by coupling to light in the waveguide, the plasmonic resonator may be merely scattering this light. Our initial data is very promising, and more experimentation will be performed to confirm that we are observing plasmonic coupling.

		
<p>Figure 14: Channel filled with fluorescent dye. Fluorescent arc lamp illumination.</p>	<p>Figure 15: Same channel, seconds later. Only laser illumination through waveguide (shown by red dotted lines).</p>	<p>Figure 16: Same channel, a minute later using fluorescence arc lamp illumination with contrast adjusted. Plasmonic stripe is clearly visible.</p>

5. DISCUSSION

There are two main results. First is the successful integration of micro-/nanofluidics, waveguides, and metallic nanostructures into a single fabrication process. The second result is the effectiveness for the initial application of this process – a nanofluidic DNA sensing chip with plasmonic readout. Figure 17 shows tagged DNA flowing through a stretch funnel in one of our chips.

A process has been presented for fabrication of devices with nanofluidic channels, integrated optical waveguides and metallic nano-plasmonic resonators. A variety of polymer and anodic wafer bonding techniques were used to make chips, with the CYTOP polymer bond process ultimately chosen for strong adhesion and minimal light scattering. This technology can be used to create sensor chips for detecting single fluorophore molecules with a very narrow detection zone, limited only by plasmonic resonator width.

The Direct Linear Analysis application is the subject of continuing research. Reduced scattering and enhanced resolution will increase the performance of these chips. Further testing will be necessary to determine the ultimate effectiveness of our device in the field of single molecule DNA sensing.

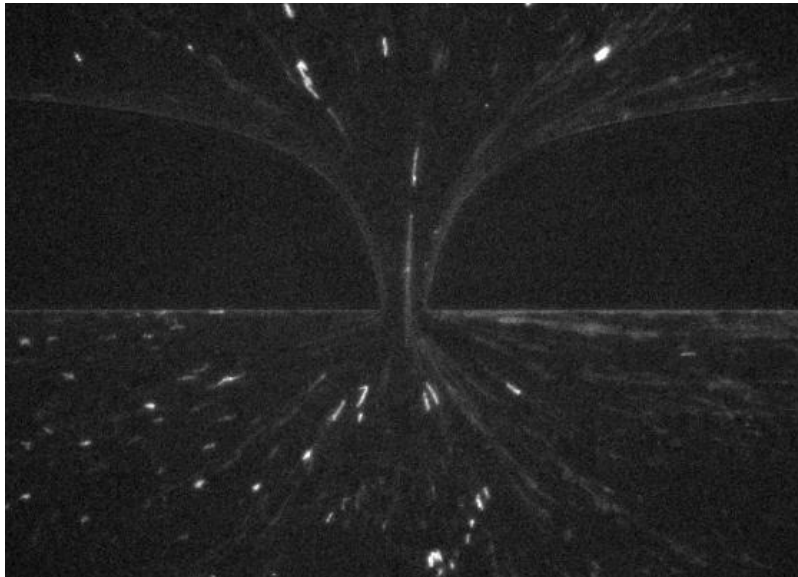


Figure 17. Fluorescent tagged DNA flowing through a hydrodynamic stretch funnel at 4.7 atm. pressure.

6. ACKNOWLEDGEMENTS

The authors would like to thank Draper Laboratory, US Genomics and the Harvard/DARPA N/MEMS MIPS center for supporting this research, and the MIT SEBL for e-beam nanolithography.

7. REFERENCES

- [1] Chan, E. F. *US Patent No. 6,355,420* (1998).
- [2] Neumann, T., Johansson, M.-L., Kambhampati, D., & Knoll, W. "Surface-plasmon fluorescence spectroscopy", *Advanced Functional Materials*, 12 (9), 575-586 (2002).
- [3] Raether, H. (1988). *Surface plasmons on smooth and rough surfaces and on gratings*. Berlin: Springer-Verlag.
- [4] <http://www.invitrogen.com/site/us/en/home/References/Molecular-Probes-The-Handbook/tables.html>
- [5] Kim, J. M., & S.Doyle, P. "Design and simulation of a DNA electrophoretic stretching device" *Lab on a Chip*, 213-225 (2007).
- [6] A. Han, K.W. Oh, S. Bhansali, H. Thurman-Henderson, and C.H. Ahn, "A Low Temperature Biochemically Compatible Bonding Technique Using Fluoropolymers for Biochemical Microfluidic Systems", *MEMS 2000*, The Thirteenth Annual International Conference on Micro Electro Mechanical Systems, 2000, pp. 414-418.
- [7] K. W. Oh, A. Han, S. Bhansali and C.H Ahn, "A low-temperature bonding technique using spin-on fluorocarbon polymers to assemble microsystems" *J. Micromech. Microeng.* 12 (2002) pp. 187-191.
- [8] N. Fong, P. Berini, R.N. Tait "Fabrication of surface plasmon waveguides on thin CYTOP membranes", *J. Vac. Sci. Technol. A* 27(4) Jul/Aug 2009.
- [9] Izawa, T., & Nakagome, H. (1972). "Silver Ion-exchange Glass Waveguides" *Appl. Phys. Lett.*, 21, 584-586.
- [10] Castro, J., & Geraghty, D. "Recent Advances in ion exchanged glass waveguides and devices", *Phys. Chem. Glasses: Eur. J. Glass Sci. Technol. B*, 47, 110-120 (2006).
- [11] Wohltjen, H., & Giuliani, J. F. *US Patent No. 4452624* (1984).
- [12] Kutchoukov, V., Laugere, F., Vlist, W. v., Pakula, L., Garini, Y., & Bossche, A. "Fabrication of nanofluidic devices using glass-to-glass anodic bonding", *Sensors and Actuators A*, 521-527 (2004).
- [13] Berthold, A., Nicola, L., Sarro, P., & Vellekoop, M. "Glass-to-glass anodic bonding with standard IC technology thin films as intermediate layers" *Sensors and Actuators A*, 82, 224-228 (2000).
- [14] Tong, Q., & Gosele, U. *Semiconductor wafer bonding: science and technology*, (New York, John Wiley, 1998).
- [15] Huber, D., & Pennathur, S. Chips & Tips: "Microfabrication design guidelines for glass micro- and nano-fluidic devices". *Lab on a Chip* (2008, April 18).